J. Membrane Biol. 68, 191–206 (1982)

The Journal of
Membrane Biology

Effects of Variation of Ion and Methylation of Carrier on the Rate Constants of Macrotetralide-Mediated Ion Transport in Lipid Bilayers

Raynald Laprade, François Grenier, Jean-Yves Lapointe, and Sylvie Asselin

Département de Physique, Université de Montréal, Montréal, Québec, Canada H3C 3J7

Summary. The effects of methylation on the rate constants of carrier-mediated ion transport have been studied on monoolein-decane bilayers with K^+, Rb^+, NH_4^+, and Tl^+ ions, using the series of homologue carriers, nonactin, monactin, dinactin, trinactin, and tetranactin, each member of the series differing from the previous one by only one methyl group. Measurements of the amplitude and time constant of the current relaxation after a voltage jump over a large domain of voltage and permeant ion concentration, together with a computer curve-fitting procedure, have allowed us, without the help of steady-state current-voltage data, to deduce and compare the values of the various rate constants for ion transport: formation (k_{Ri}) and dissociation (k_{Di}) of the ion-carrier complex at the interface, translocation across the membrane interior of the carrier (k_s) and the complex (k_{is}). With the additional information from steady-state low-voltage conductance measurements, we have obtained the value of the aqueous phase-membrane and torus-membrane partition coefficient of the carrier (γ_s and Γ_s). From nonactin to tetranactin with the NH_4^+ ion, k_{is}, and γ_s are found to increase by factors of 5 and 3, respectively, k_{Di} and Γ_s to decrease respectively by factors 8 and 2, while k_{Ri} and k_s are practically invariant. Nearly identical results are found for K^+, Rb^+, and Tl^+ ions. k_{Ri}, k_s and k_{is} are quite invariant from one ion to the other except for Tl^+ where k_{Ri} is about five times larger. On the other hand, k_{Di} depends strongly on the ion, indicating that dissociation is the determining step of the ionic selectivity of a given carrier. The systematic variations in the values of the rate constants with increasing methylation are interpreted in terms of modifications of energy barriers induced by the carrier increasing size. Within this framework, we have been able to establish and verify a fundamental relationship between the variations of k_{is} and k_{Di} with methylation.

Key words ion transport · carriers · lipid bilayers · kinetics · nonactin · methylation · macrotetralides

Introduction

The purpose of this work is to investigate in a systematic way the influence of ion and molecular variations of the ionophore on the rate constants of carrier-mediated ion transport through lipid bilayers. Our goal through this study is to gain more insight at the molecular level on the fundamental mechanisms of ion permeation through membranes. The macrotetralide actins (nonactin to tetranactin) constitute a particularly well-suited series of molecules since each homologue differs from the preceding one by only one methyl group.

Since their early identification as ion translocators in lipid bilayers (Mueller & Rudin, 1967; Pressman, Harris, Jaeger & Johnson, 1967; Eisenman, Ciani & Szabo, 1968; Tosteson, 1968), these molecules have been the subject of various investigations on lipid bilayers, which all contributed to confirm their role as mobile ion carriers. Earlier works were confined to steady-state potential and conductance measurements, which allowed the determination of ionic permeability ratios in terms of a model where the interfacial reactions were assumed at equilibrium (Eisenman et al., 1968; Szabo, Eisenman & Ciani, 1969; Szabo et al., 1973; Eisenman et al., 1973). Then with Markin, Kristalik, Liberman, and Topaly (1969) followed by Läuger and Stark (1970), by Hladky (1972), by Ciani, Eisenman, Laprade, and Szabo (1973*a*) and by Ciani, Laprade Eisenman, and Szabo (1973*b*), theoretical frameworks in the steady-state were available where diffusion of the complexes across the membrane interior was no longer the rate-limiting step. One entered the "kinetic era." The theoretical expectations of these models sufficed to account for an important body of membrane steady-state data (zero-current potential and conductance, current-voltage relationship) and allowed one in appropriate systems to deduce interesting combinations of kinetic parameters (Stark & Benz, 1971; Ciani et al., 1973*a*; Benz & Stark, 1975; Feldberg & Kissel, 1975; Hladky, 1975*a*; Laprade, Ciani, Eisenman & Szabo, 1975; Krasne & Eisenman, 1976).

However, it was only with the introduction of the voltage-clamp relaxation technique (Stark, Ketterer, Benz & Läuger, 1971) that one could get at the individual values of the rate constants. Laprade et al. (1975), on glyceryl-dioleate/decane membranes,

0022-2631/82/0068-0191 $03.20

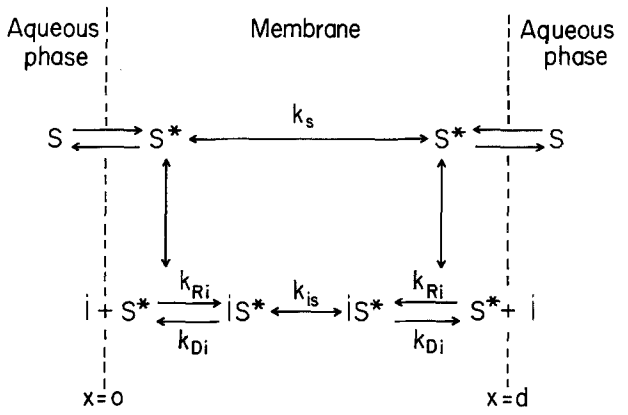

Fig. 1. Schematic diagram of the processes involved in carrier-mediated ion transport

Benz and Stark (1975), on monoglyceride/decane membranes, and Hladky (1975*b*), on glyceryl-monooleate/hexadecane membranes, deduced the individual rate constants for trinactin-mediated transport with various ions. Relaxation studies were also conducted with nonactin by Hladky (1975*b*) and by Benz and Stark (1975) for the series nonactin through trinactin with the NH_4^+ ion. Although used primarily as a steady-state method, the charge pulse technique also allowed Feldberg and Kissel (1975) to estimate the rate constants for the series nonactin through trinactin with the NH_4^+ ion.

However, even with all the existing data obtained from relaxation studies, it is not possible to build a complete kinetic characterization with the whole series from nonactin to tetranactin on the same type of membrane, in the same experimental conditions, and with a good variety of ions, which would allow a useful and unambiguous comparison of the rate constants amongst the different homologues and ions[1].

So it is the purpose of this work to report such a kinetic characterization and comparison. The use of an averaging system in the experimental set-up has allowed us to obtain data on ion-carrier combinations and in concentration ranges that could not be studied previously. In addition, we present results on the carrier tetranactin and the thallium ion which had never heretofore been reported. Moreover, a novel way of deducing the individual rate constants will be introduced, which uses solely relaxation data in contrast with the standard approach which relies also on steady-state current-voltage data.

[1] The reader interested in a detailed and critical review of carriers is referred to the excellent and recent one by Hladky (1979*b*).

Theory

The transport model we will use is schematized in Fig. 1 and corresponds to the widely accepted model for carrier-mediated ion transport introduced by Markin et al. (1969), Läuger and Stark (1970) and Stark et al. (1971). This model is essentially identical to that of Ciani (Ciani et al., 1973*a*; Laprade et al., 1975) with the omission of the complex partition process. The notation used here is that of Hladky's recent review (Hladky, 1979*b*), which is a slightly modified version of that of Läuger and Stark (1970).

Time Dependence of the Electric Current

For such a system, it has been shown in an Eyring type of treatment (Stark et al., 1971; Hladky, 1975*b*; Laprade et al., 1975) that the time course of the current after a voltage jump is given by

$$I(t) = I_\infty (1 + \alpha_1 e^{-t/\tau_1} + \alpha_2 e^{-t/\tau_2}) \tag{1}$$

where I_∞ is the steady-state or stationary current, which for the case of a monovalent cation and a carrier added via the aqueous phase is given by

$$I_\infty = F d \gamma_s \frac{k_{Ri}}{k_{Di}} k_{is} \frac{c_s^a c_i}{[1 + K c_i]} \frac{\sinh(u/2)}{[1 + A \cosh(u/2)]}. \tag{2}$$

α_1 and α_2 are the relaxation amplitudes, while τ_1 and τ_2 are the relaxation time constants, which are given by

$$1/\tau_1 = a - b \tag{3}$$

$$1/\tau_2 = a + b \tag{4}$$

where

$$2a = 2k_{is} \cosh(u/2) + k_{Di} + 2k_s + k_{Ri} c_i \tag{5}$$

$$2b = [(2k_{is} \cosh(u/2) + k_{Di} - 2k_s - k_{Ri} c_i)^2 + 4 k_{Ri} c_i k_{Di}]^{\frac{1}{2}} \tag{6}$$

$$\alpha_1 = \frac{A}{2} \cosh(u/2) + B \tag{7}$$

$$\alpha_2 = \frac{A}{2} \cosh(u/2) - B \tag{8}$$

$$B = \frac{\cosh(u/2)}{4b} [A(k_{Ri} c_i + k_{Di} + 2k_s - 2k_{is} \cosh(u/2)) - 4k_{is}] \tag{9}$$

$$\alpha_1 + \alpha_2 = A \cosh(u/2) = \alpha_T \tag{10}$$

$$A = \frac{k_{is}}{k_{Di}} \left(2 + \frac{k_{Ri} c_i}{k_s}\right) \tag{11}$$

$$u = \frac{FV}{RT}. \tag{12}$$

In the above expressions, F is the Faraday, d, the membrane thickness, γ_s, the aqueous phase-membrane partition coefficient, c_i, the permeant ion concentration, c_s^a, the total aqueous carrier concentrations, K, the aqueous phase ion-carrier complexation constant, and V, the applied voltage.

Zero-Current Conductance

In the limit of low applied voltages and thus low currents, we obtain from Eq. (2) the so-called zero-current conductance (Szabo et al., 1969; Läuger & Stark, 1970)

$$G_o^a = \lim_{V\to 0} \frac{I_\infty}{V} = \frac{F^2 d\gamma_s}{2RT} k_{is} \frac{k_{Ri} c_s^a c_i}{k_{Di}(1+Kc_i)(1+A)} \tag{13}$$

where the superscript "a" refers to the carrier added to the aqueous phase. In the case where the carrier is added to the lipid phase (l) and for small membranes which are torus-buffered (Hladky, 1972, 1973; Benz, Stark, Janko & Läuger, 1973) we have

$$G_o^l = \frac{F^2 d}{2RT} \Gamma_s k_{is} \frac{k_{Ri}}{k_{Di}} \frac{c_s^l c_i}{(1+A)} \tag{14}$$

where Γ_s is the torus-membrane partition coefficient.

Materials and Methods

Black lipid membranes were formed from a 25-mg/ml solution in *n*-decane of monoolein obtained from Sigma. Membranes were formed according to previously published method (Szabo et al., 1969) on a Teflon partition separating two aqueous compartments of 20 ml volume each. The diameter of the aperture in the Teflon partition for the relaxation experiments was either 0.6 or 1 mm. The same aperture diameters were used for the steady-state zero-current conductance measurements where the carrier was added via the lipid phase. For the conductance measurements where the carrier was added via the aqueous phase the aperture diameter was 4.3 mm. In the latter case, in order to minimize adsorption of the carrier to the Teflon walls, the membrane was formed on a Teflon disc separating two glass compartments (Laprade, Grenier & Asselin, 1979)[2]. The measurements were carried out at room temperature which was kept constant at 22.5 ± 0.5 °C. Nonactin was a gift from Barbara Sterns of Squibb and Hans Bickel of Ciba-Geigy; monactin, dinactin, and trinactin were gifts from Hans Bickel, and tetranactin was a gift from W. Simon and from K. Ando. Small volumes of stock ethanol solutions of the carrier ($10^{-5}-10^{-3}$ M) were added either to the aqueous or the lipid phase. The final concentration of ethanol in the aqueous phase never exceeded 1%. When the carrier was added to the lipid phase, the ethanol from the appropriate stock solution was first evaporated and then replaced by an equal volume of lipid solution. Aqueous salt solutions were chlorides of the different ions except for thallium, where it was acetate. Ionic strength was kept constant at 1 M with LiCl except for thallium, where the salt was $LiNO_3$.

[2] Laprade, R., Grenier, F., Asselin, S. Lateral diffusion of ion carriers in lipid bilayers. *Manuscript in preparation*

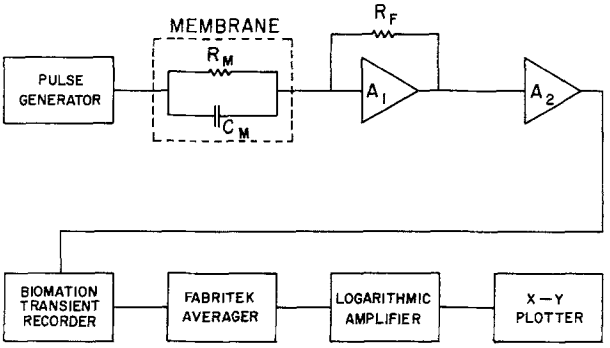

Fig. 2. Schematic diagram of the experimental set-up for the electrical relaxation studies

The conductance measurements were performed as in previous studies (Szabo et al., 1969; Laprade et al., 1975). For relaxation experiments, we waited about 15 min after the blackening of the membrane before recording the current transient decay since we had observed a gradual decrease of the time constant during the first 10 min. A schematic diagram of the experimental set-up is shown in Fig. 2. Voltage pulses of about 1 msec duration were supplied by a pulse generator with a rise time of 10 nsec (Hewlett-Packard 8005A). A CA3040 wideband amplifier (RCA) with a constant open loop gain of 30 up to 100 MHz was used as a current amplifier with feedback resistors of 5.4 or 22.4 kΩ; its output was amplified by a second CA3040 in an open loop configuration. A Biomation 805 dual time base transient recorder was used as a buffer to an averager (Fabri-Tek Instruments, Inc., model 1072). Signal repetition rates varied around 200 Hz, and between 1024 and 8196 samples were taken on the same membrane. The first 90% of the current decay was recorded with the first time base at a setting allowing maximum resolution and the last 10% with the second time base at a ten times slower setting, thus allowing the decay to be totally completed by the end of the recording. The output of the averager corresponding to $(I(t) - I_\infty)$, where I_∞ is the steady-state current, was fed to a logarithmic amplifier, whose output was displayed on an $x-y$ plotter. The time constant of the exponential decay could be read directly from the slope of the straight line on the $x-y$ plotter, the intercept at $t=0$ giving the difference between instantaneous and steady-state current. Obviously the relaxation current could be relied upon only after the capacitive transient, whose time constant for the smallest membranes was less than 200 nsec. The procedure has allowed us to measure relaxations of small amplitudes and short time constants with increased precision using lower carrier concentrations.

Numerical Methods

The procedure we have used for the analysis of the rate constants from the relaxation data requires curve fitting the theoretically predicted values (X_{theor}) of the amplitudes and time constants to the experimentally measured ones (X_{exp}). In order to obtain the values of the parameters k_{is}, k_s, k_{Ri}, and k_{Di}, which would give the optimum fit between experimental quantities and predicted ones, we have used a least-squares fir program on a digital computer. This program, starting with hand-calculated initial guesses (*c.f.* Results) for the values of the parameters varies them until it finds a minimum (in four dimensions) for the sum of $[(X_{exp} - X_{theor})/X_{exp}]^2$ for all the points. In this procedure, it is the relative difference which is minimized, so that each point is then given the same importance.

Table 1. Values of τ_{obs} and α_{obs} for trinactin and tetranactin with NH_4^+

V (mV)	Trinactin c_i (M)					Tetranactin c_i (M)				
	10^{-2}	3×10^{-2}	10^{-1}	0.5	1	10^{-2}	3×10^{-2}	10^{-1}	0.5	1
	τ_{obs} (μsec)									
10	32.5	32.0	37.5	42.3	43.0	26.9	29.3	29.5	29.1	27.8
25	30.1	30.9	35.4	40.0	41.0	24.6	26.8	28.0	27.6	26.0
50	25.0	26.3	30.5	33.6	33.9	20.4	20.6	22.5	22.5	21.6
100	15.3	16.3	19.1	20.6	20.5	11.6	11.9	12.6	12.7	11.9
150	8.8	9.6	11.5	12.0	11.6	6.0	5.9	6.2	6.9	6.2
	α_{obs}									
10	2.5	2.5	2.3	3.4	5.3	7.3	7.8	7.8	13.2	18.0
25	2.8	2.7	2.4	3.9	5.8	8.1	8.3	8.8	14.5	20.6
50	3.7	3.4	3.1	4.7	7.4	10.8	11.4	12.0	18.5	26.2
100	7.4	6.7	6.0	8.9	14.9	26.8	26.0	28.9	44.9	58.0
150	21.1	15.7	12.8	18.9	35.0	115	137	136	153	191

Values at $c_s^a = 5\times10^{-9}$ M

Results

Relaxation amplitudes and time constants, α_{obs} and τ_{obs}, were measured at ion concentrations ranging in most cases from 10^{-2} to 1 M, and, in some instances, up to 3 M, and for voltage jumps from 10 to 150 mV. These measurements were carried for the whole series of nonactin and its homologues with NH_4^+, K^+, Rb^+, and Tl^+ ions. In all cases, aside from the early capacitive transient, only one exponential relaxation could be detected (τ_{obs}, α_{obs}). In general, we can state that at low voltage as ion concentration is decreased, τ_{obs} and α_{obs} decrease and approach a finite limiting value, and as ion concentration is increased, α_{obs} increases linearly; finally, at a given ion concentration, τ_{obs} strongly decreases with voltage while α_{obs} increases. Typical results are shown in Table 1, and Figs. 3 and 4, while complete data are presented in Appendix B. Accordingly, as described by Hladky (1975*b*, 1979*b*), τ_{obs} and α_{obs} were identified with the slower relaxation τ_1 and α_1, whose expressions are given in Eqs. (3) and (7).

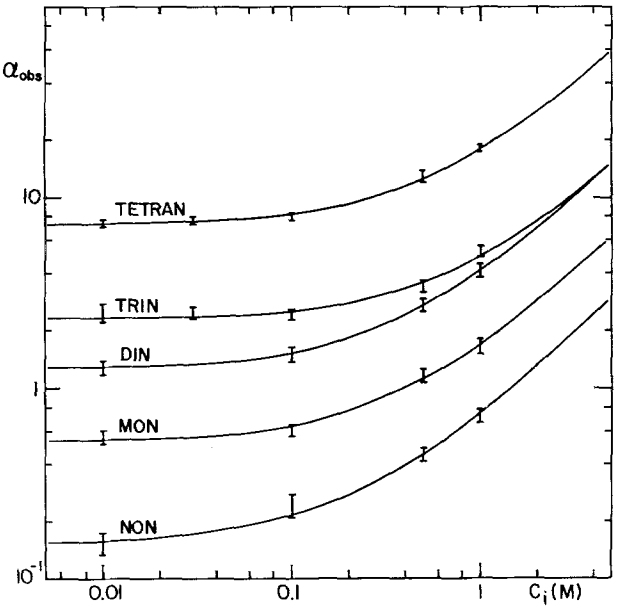

Fig. 3. Measured amplitude of relaxation, α_{obs}, at 10 mV as a function of ion concentration for the whole series of macrotetralides. The theoretical curves have been drawn according to Eq. (17). Vertical bars indicate scatter

Determination of the Rate Constants

From the above considerations, we can obtain in the limit of low voltage good estimates for the values of the rate constants k_{is} and k_{Di} and the ratio k_{Ri}/k_s (Hladky, 1979*b*). Indeed at low ion concentration

$$\tau_{obs} \simeq \tau_1 \simeq 1/(2k_{is} + k_{Di}) \tag{15}$$

and

$$\alpha_{obs} \simeq \alpha_1 + \alpha_2 = 2k_{is}/k_{Di} \tag{16}$$

from which separate values of k_{is} and k_{Di} can be calculated. At higher ion concentration (*c.f.* Fig. 3)

$$\alpha_{obs} \simeq \alpha_1 + \alpha_2 = (k_{is}/k_{Di})(2 + k_{Ri}c_i/k_s) \tag{17}$$

the slope of which as a function of ion concentration gives, from the knowledge of k_{is}/k_{Di}, the ratio k_{Ri}/k_{is}; we are left with only one unknown (k_{Ri} or k_s) which can be calculated in principle from the value of τ_{obs} at higher ion concentration and voltage. In-

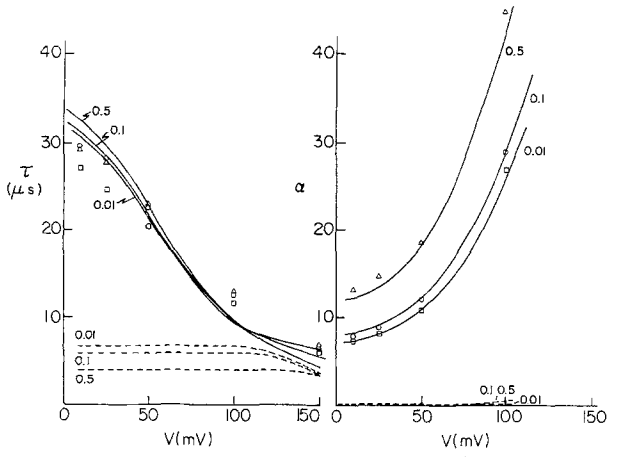

Fig. 4. An example of curve-fitting for the tetranactin-NH_4^+ ion-carrier complex. The open symbols represent the experimental data: squares, 0.01 M; circles, 0.1 M; and triangles, 0.5 M. The solid curves represent theoretical curves corresponding to the best-fit of τ_1 and α_1 to the experimental data, using the values of Table 2 for the rate constants. The dashed curves represent the corresponding theoretical values of τ_2 and α_2

spection of Fig. 3 clearly shows that Eq. (17) is very well followed, which strongly suggests that both ratios, k_{is}/k_{Di} and k_{Ri}/k_s, are constants independent of c_i. This also constitutes a strong indication that the individual rate constants are independent of c_i, since indeed it would be highly fortuitous that k_{Ri} and k_s, for example, would vary in a parallel way. This finding for all macrotetralides, which confirms the observations of Hladky (1975*b*) for nonactin and trinactin, is very interesting since it was shown for valinomycin (Knoll & Stark, 1975; Benz & Läuger, 1976) and the enniatins (Benz, 1978) that, although k_{is} and k_{Di} seemed fairly constant with c_i, k_s showed a slight decrease, while k_{Ri} showed a strong one, with increasing ion concentration.

In order to obtain values for the rate constants which would give the optimum fit to τ_{obs} and α_{obs} over the extensive experimental range studied, the above estimates were used as initial guesses in a computer curve-fitting program (*see* Numerical Methods). Interestingly, in all cases, the final values for k_{is}, k_{Di}, and the ratio k_{Ri}/k_s came out very close to the initial values. Only in the separate values of k_{Ri} and k_s were there significant differences. Using these values in the expressions for α_2 and τ_2, we have verified that indeed this faster relaxation process could not be detected experimentally.

In addition to the curve-fitting procedure, the present method of obtaining the separate values for the rate constants differs from the usual method (Stark et al., 1971; Benz et al., 1973; Gambale, Gliozzi & Robello, 1973; Benz & Stark, 1975; Hladky, 1975*b*; Laprade et al., 1975), in that it relies solely on relaxation data. Thus, it does not make use of the ratios k_{is}/k_{Di} and k_{Ri}/k_s determined from current-voltage data, which, as was pointed out by Hladky (1979*b*), can be much in error due to the particular form of the equation and the inadequacy of the voltage function to describe the current-voltage relationship.

Table 2 presents the values of the individual rate constants obtained from independent curve-fittings for each ion-carrier combination over the whole range of voltage and ion concentration. Some of the results for the NH_4^+ ion have been reported earlier in a preliminary form (Laprade, Grenier & Asselin, 1978). Table 3 shows some useful and interesting ratios of the rate constants calculated from the values of Table 2. For Rb^+ with nonactin and monactin, the data at low ion concentration was not sufficient to allow reasonably reliable values to be obtained from our method of analysis. For each ion-carrier combination, we also present in Table 2 the mean percent difference between predicted and data values ($\bar{\Delta}\% = 100[\Sigma|(X_{exp} - X_{theor})|/X_{exp}]/n$, where n is the number of points), each data point being the mean of about three different measurements. We can see that the fits are quite good, especially those for the highest homologues and preferred ions (*c.f.* Fig. 4), for which we obtain larger time constants and amplitude of relaxations that are easier to measure. Indeed, we can state that, in general, the quality of the fit parallels quite closely the quality of the data, the latter reflecting to a large extent variations from one membrane to the other (Hladky, 1975*b*). However, one may ask what is the reliability on the values of the rate constants so determined. In order to have some idea on this matter, we have fixed the value of one rate constant and allowed the others to vary at will in order again to get the best fit; we have then calcuated $\bar{\Delta}\%$ for different fixed values of this rate constant. We have done this for the four rate constants k_{is}, k_{Di}, k_{Ri}, k_s, and the ratio k_{Ri}/k_s; the results for trinactin-NH_4^+ are shown in Fig. 5 where $\bar{\Delta}\%$ is plotted as a function of the ratio of the fixed over the optimum value of the rate constant. Quite similar curves are obtained for other ion-carrier combinations. It can be seen that the minimum is quite sharp in the case of k_{is}, k_{Di}, and the ratio (k_{Ri}/k_s). A much shallower minimum is seen for k_{Ri} and k_s, although it is clear that k_s has to be greater than a certain value. This means that the values of k_{is}, k_{Di}, and the ratio k_{Ri}/k_s are very well determined, while the separate values of k_{Ri} and k_s could be given with certitude only a minimum value. This finding corresponds to what is expected since Eqs.

Table 2. Rate constants from nonactin to tetranactin

			NH_4^+	K^+	Rb^+	Tl^+
Tetran	k_{is}	(sec^{-1})	1.44×10^4	1.69×10^4	2.03×10^4	1.47×10^4
	k_s	(sec^{-1})	6.13×10^4	7.24×10^4	1.14×10^5	1.39×10^5
	k_{Ri}	($M^{-1} - sec^{-1}$)	1.79×10^5	1.27×10^5	2.93×10^5	6.6×10^5
	k_{Di}	(sec^{-1})	4.06×10^3	1.80×10^4	9.01×10^4	1.62×10^4
	$\bar{\Delta}\%$		6.6	8.6	10.3	15.1
Trin	k_{is}		8.98×10^3	9.00×10^3	9.38×10^3	6.39×10^3
	k_s		9.20×10^4	1.17×10^5	7.84×10^4	1.99×10^5
	k_{Ri}		1.70×10^5	2.80×10^5	1.07×10^5	1.22×10^6
	k_{Di}		9.00×10^3	6.47×10^4	1.68×10^5	4.1×10^4
	$\bar{\Delta}\%$		16.8	12.8	10.8	18.4
Din	k_{is}		7.74×10^3	7.19×10^3	8.75×10^3	4.49×10^3
	k_s		6.37×10^4	6.98×10^4	7.04×10^4	1.82×10^5
	k_{Ri}		3.16×10^5	1.68×10^5	1.76×10^5	1.07×10^6
	k_{Di}		1.35×10^4	1.24×10^5	4.94×10^5	6.00×10^4
	$\bar{\Delta}\%$		15.0	22.9	9.9	11.7
Mon	k_{is}		5.09×10^3	6.8×10^3		2.13×10^3
	k_s		6.60×10^4	1.7×10^5		7.65×10^4
	k_{Ri}		1.70×10^5	2.8×10^5		8.03×10^5
	k_{Di}		1.98×10^4	1.95×10^5		1.33×10^5
	$\bar{\Delta}\%$		13.6	20.5		16.8
Non	k_{is}		2.86×10^3	5.9×10^3		1.77×10^3
	k_s		8.6×10^4	6.3×10^4		1.26×10^5
	k_{Ri}		3.7×10^5	2.3×10^4		8.36×10^5
	k_{Di}		3.17×10^4	1.6×10^5		3.46×10^5
	$\bar{\Delta}\%$		16.5	18.9		25.1

Table 3. Values of the ratios k_{Ri}/k_{Di}, k_{Ri}/k_s and k_{is}/k_{Di} from nonactin to tetranactin

		NH_4^+	K^+	Rb^+	Tl^+
Tetran	k_{Ri}/k_{Di} (M^{-1})	44.1	7.1	3.25	40.7
	k_{Ri}/k_s (M^{-1})	2.92	1.75	2.57	4.75
	k_{is}/k_{Di}	3.55	0.94	0.23	0.91
Trin	k_{Ri}/k_{Di}	19.9	4.32	0.64	29.8
	k_{Ri}/k_s	1.85	2.39	1.36	6.13
	k_{is}/k_{Di}	1.0	0.14	0.056	0.16
Din	k_{Ri}/k_{Di}	23.4	1.35	0.36	17.8
	k_{Ri}/k_s	4.96	2.4	2.5	5.88
	k_{is}/k_{Di}	0.57	0.058	0.018	0.075
Mon	k_{Ri}/k_{Di}	8.58	1.44		6.07
	k_{Ri}/k_s	2.57	1.65		10.5
	k_{is}/k_{Di}	0.26	0.035		0.016
Non	k_{Ri}/k_{Di}	11.6	0.14		2.42
	k_{Ri}/k_s	4.30	0.37		6.63
	k_{is}/k_{Di}	0.09	0.037		0.0051

Calculated from the values in Table 2.

(15), (16), and (17), which gave the estimates for k_{is}, k_{Di}, and k_{Ri}/k_s are very good approximations, while it was shown by Benz et al. (1973) that separate values for k_{Ri} and k_s could be obtained only when α_{obs} was significantly less than α_T, which is obviously the case here only at the highest voltages. Nevertheless in the following, additional arguments, mostly based on steady-state measurements, will be given that should justify a good degree of confidence in the values of k_{Ri} and k_s reported in Table 2.

It should be stated that the values of the rate constants we have found do not depend critically on the particular voltage dependence of the translocation rate of the complex we have used and which appears in the different equations as $k_{is}\cosh(u/2)$. Indeed using the weaker voltage function $k_{is}\cosh(nu)$ for the rate of transfer of the complex (Hladky, 1975*b*; Knoll & Stark, 1975; Laprade et al., 1975), we have found with the NH_4^+ ion and the whole series of actins, letting n be an additional adjustable parameter ($0.37 < n < 0.44$), that k_{is} increases by less than 10%, while k_{Di} decreases by less than 3%. Moreover, the voltage dependence of the rate constants is of little importance here since we are more interested in the variations of the rate constants when going from one carrier to the other or from one ion to the other, than in the precise absolute value of the rate constants which will always be dependent on the assumptions made. This is clearly seen in Appendix A where rate constants are derived in the limit of low applied voltage, taking

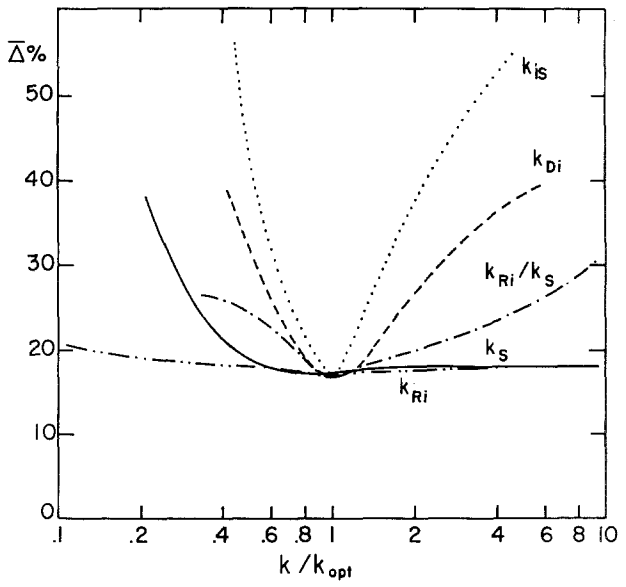

Fig. 5. Illustration of the reliability on the values of the rate constants corresponding to the optimum fit for trinactin-NH_4^+. The value of a single rate constant is fixed at a value different from the optimum one and the other three are allowed to vary in order to get a minimum in the mean relative error between predicted and experimental points ($\bar{\Delta}\%$). $\bar{\Delta}\%$ is plotted as a function of the ratio k/k_{opt} of the fixed over the optimum value

into account their voltage dependence. Indeed, although the absolute values might be different from those in Table 2, the variations we are interested in are not significantly altered.

Ratios of k_{Ri} from Conductance Measurements

As stated before, although the ratio k_{Ri}/k_s is rather well defined, the separate values of k_{Ri} and k_s do not appear as clearly defined. Nevertheless, the fact that k_s for a given carrier turns out to be the same for different ions legitimates some confidence in the values of these two constants. However, the reliability of these values can be checked indirectly with data from steady-state conductance measurements at low ion concentration. For two different ions with a given carrier, we have

$$\frac{G_0(j)}{G_0(i)}=\frac{k_{Rj}}{k_{Ri}}\frac{k_{Di}}{k_{Dj}}\frac{k_{js}}{k_{is}}\frac{(1+2k_{is}/k_{Di})}{(1+2k_{js}/k_{Dj})}. \tag{18}$$

Since k_{Di}, k_{Dj}, k_{is}, and k_{js} as well as the ratio $G_0(j)/G_0(i)$ are known with a good degree of reliability, one can calculate the ratio (k_{Rj}/k_{Ri}) and compare it with that obtained from the relaxation analysis. Table 4 shows such a comparison. The conductance ratios that have been used and appear in Table 5 have been obtained on small area membranes with the carrier added to the lipid at a concentration varying between 10^{-5} and 10^{-4} M. The ratios for K^+ and Rb^+ are not much different from unity, and we can see from the comparison of columns I and II that the agreement is good within about a factor of two. It is interesting to see also that the k_{Ri} values for Tl^+ which were systematically larger than those for NH_4^+, K^+ or Rb^+ ions, either from the value of the ratio k_{Ri}/k_s in Table 3 or their separate value in Table 2, are also larger here from comparison of the conductance levels.

Table 4. Comparison of the ratios $k_{Ri}/k_{RNH_4^+}$ of the relaxation analysis with those calculated from steady-state conductance data

	Mon		Din		Trin		Tetran	
	I	II	I	II	I	II	I	II
K^+	1.65	0.84	0.53	2.2	1.65	1.44	0.71	1.53
Rb^+			0.56	2.2	0.63	1.19	1.63	2.53
Tl^+	4.72	12.4	3.4	7.1	7.18	7.44	3.7	4.11

I: Calculated from the values in Table 2.
II: Calculated from Eq. (18) using the values of k_{is} and k_{Di} of Table 2 and the values of the ratios $G_0(i)/G_0(NH_4^+)$ of Table 5.

Table 5. Values of the ratios $G_0(i)/G_0(NH_4^+)$ at low ion concentration

	Mon	Din	Trin	Tetran
K^+	0.22	0.42	0.47	1.14
Rb^+	0.09	0.14	0.18	0.90
Tl^+	1.12	1.89	2.56	3.57

Determination of the Partition Coefficients γ_s and Γ_s

Since all other parameters are known, γ_s and Γ_s can be obtained from conductance measurements at low ion concentration with the help of Eqs. (13) or (14), depending on whether the carrier is added to aqueous phase or to the lipid-forming solution. In the former case, in order to minimize the effect of exchange of carrier between the membrane and the torus and thus to be the closest possible to the equilibrium concentration of the carrier in the membrane (Hladky, 1973; Laprade et al., 1979), large area membranes have been used (0.15 cm^2; *see also* Methods). Conversely, in the latter case, in order to be torus buffered (Hladky, 1973), we have used small area membranes (5×10^{-3} cm^2). The first and last rows of Table 6 give the values of γ_s and Γ_s, calculated from Eqs. (13) and (14), respectively, using the values for the rate constants from Table 2. It can be seen that γ_s increases only slightly from nonactin to tetranactin while Γ_s decreases almost by the same amount. This small increase in γ_s with methylation

Table 6. Calculated partition coefficients γ_s and Γ_s[a]

	Non	Mon	Din	Trin	Tetran
γ_s[b]	2.4×10^5	2.6×10^5	7.4×10^5	5.1×10^5	7.4×10^5
γ_s[c]	2×10^5	1.6×10^5	6.7×10^5	4.2×10^5	3.7×10^5
Γ_s[d]	9.4	10.7	6.2	7.5	5.8

[a] Calculated from NH_4^+ data and for $d=5\times10^{-7}$ cm.

[b] From Eq. (13) using values of the rate constants from Table 2 and the following respective values of G_0 (Siemen-cm^{-2}) from nonactin to tetranactin, measured on large area membranes (4 mm diameter) and at $c_i=10^{-2}$ M, $c_s^T=10^{-8}$ M: 6.6×10^{-4}, 7.1×10^{-4}, 5.9×10^{-3}, 3.3×10^{-3}, and 5.8×10^{-3}.

[c] From Eq. (19) using the following respective values (s) for τ from nonactin to tetranactin: 170, 130, 560, 350, 310. $D_s=3\times10^{-6}$ cm^2-sec^{-1}, $\delta=10^{-2}$ cm, $d=5\times10^{-7}$ cm.

[d] From Eq. (14) and the following respective values (Siemen-cm^{-2}) for G_0 from nonactin to tetranactin measured on small area membranes (0.8 mm diameter) and at $c_i=10^{-2}$ M, $c_s^l=10^{-4}$ M: 2.4×10^{-4}, 2.92×10^{-4}, 4.93×10^{-4}, 4.25×10^{-4}, and 4.32×10^{-4}.

is in agreement with the finding of Benz and Stark (1975), although the values for γ_s found here are about one order of magnitude higher than those found by Benz and Stark (1975). This is due mainly to the fact that our values of conductance are about one order of magnitude higher than theirs. This difference can be explained by the fact that these authors have used smaller area membranes and a Teflon cell on the walls of which an important fraction of the carrier is lost by adsorption (Laprade et al., 1979). However, our values for G_0^l are close to those found by Hladky (1975*a*) on hexadecane bilayers and our values of Γ_s in close agreement with his for nonactin and trinactin.

Of course, the reliability on the values of γ_s and Γ_s depends on the reliability on the values of k_{is}, k_{Di}, and k_{Ri} as can be seen from Eqs. (13) or (14), k_{Ri} being again the most questionable. Interestingly, a further check is provided by an independent measurement of γ_s. For a very large area membrane and low enough ion activity, so that the number of complexes is negligible as compared to the number of free carriers, one can show (Hladky, 1973; Laprade et al., 1979)[3] that the time constant for the increase in G_0^a after addition of the carrier to the aqueous phase and the beginning of stirring is given by

$$\tau=\gamma_s\frac{d}{2}\Big/(D_s/\delta) \tag{19}$$

where d is the membrane thickness, D_s, the aqueous diffusion coefficient of the carrier, and δ, the thickness of the unstirred layer. d is assumed from the measured dielectric thickness to be 50 Å (Fettiplace, Andrews & Haydon, 1971; White, 1973; Benz, Frölich, Läuger & Montal, 1975). δ is assumed to be equal to 10^{-2} cm (Hladky, 1973). D_s is calculated[4] to be 3×10^{-6} cm^2-sec^{-1} and assumed to be the same for all the homologues. The values obtained from Eq. (19) appear in the center row of Table 6. They are strikingly similar to those of the first row which were obtained from Eq. (13) using the values of the rate constants of Table 2, thus corroborating the reliability of the latter values.

Discussion

The most striking feature of Table 2 is certainly the increase in k_{is} parallelled by the decrease in k_{Di} as a function of increasing methylation of the carrier (non → tetran) which is seen for all studied ions. Then, for all carriers, we observe a quasi-invariance in k_{is} with ion, indicating isostericity of the complexes (Eisenman, Ciani & Szabo, 1969; Eisenman et al., 1973), a fact which had been verified earlier for trinactin (Laprade et al., 1975; Benz & Stark, 1975; Hladky, 1975*b*). Finally, k_{Ri} and k_s seem to be quite invariant from one carrier to the other as well as from one ion to the other except for thallium, where k_{Ri} tends to be systematically and significantly larger. The fact that k_s does not vary from one ion to the other is not surprising since, in principle, it should be invariant; however, its constancy (within a factor of two) as a function of the ion is an indication of the internal consistency of the method of analysis.

The values of the rate constants in Table 2 agree within approximately a factor of two with the corresponding ones reported by Hladky (1975*b*) for nonactin and trinactin with NH_4^+ and K^+ ions on monooleine/hexadecane bilayers and by Benz and Stark (1975) for trinactin with NH_4^+, K^+, and Rb^+ ions on monooleine/decane bilayers. For nonactin, monactin, and dinactin with NH_4^+, our values for k_{is}, k_{Di}, and the ratio k_{Ri}/k_s still agree within a factor of two with those of Benz and Stark (1975), although for the individual values of k_{Ri} and k_s, they are about five times larger. The agreement is still good with the estimates of Feldberg and Kissel (1975) for nonactin to trinactin with NH_4^+, although our values for k_s for all homologues as well as k_{is} for the lower ones are significantly smaller.

[3] *See* footnote 2, p. 193

[4] By comparison with the tetraphenylborate molecule, for which the diffusion coefficient is 4.6×10^{-6} cm^2/sec (Skinner & Fuoss, 1964), using Stoke's law and the known value of the radii of nonactin and tetraphenylborate, 6.25 and 4.2 Å, respectively (Simon & Morf, 1973; Grunwald, Baughman & Kohnstam, 1960).

However, although the values of the constants are in the same range, the trends in k_{is} and k_{Di} as a function of carrier methylation, which though not apparent, were already contained in the results of Benz and Stark (1975), Hladky (1975*b*) and Feldberg and Kissel (1975), are much more emphasized here, due both to the larger number of homologues and ions involved and the larger differences observed in the values of the rate constants from one homologue to the other.

k_{is}

The increase of k_{is} with methylation would seem at first glance somehow surprising since one would expect, if anything, a larger complex to be slower in crossing the membrane interior (Krasne & Eisenman, 1976). However, electrostatic energy considerations may offer, as we will see, an interesting and mostly satisfactory explanation for this phenomenon. Indeed the height of the electrostatic energy barrier a complex sees, corresponds to the difference between its energy level in the middle of the membrane, $E_B(d/2)$, and that at the bottom of the well at the adsorption site near the interface, $E_B(x)$ where x is the distance from the interface. For a carrier of radius r_c and dielectric constant ε_c with an ion of radius r_i, and for a membrane of thickness d and dielectric constant ε_2 separating two aqueous phases of dielectric constant ε_1, we have, expressed in units of kT (Neumcke & Läuger, 1969; Parsegian, 1969)[5]

$$E_B(d/2) = E_{B_\infty} - \frac{2q_0}{\varepsilon_2 d} \ln \frac{2\varepsilon_1}{\varepsilon_1 + \varepsilon_2} \tag{20}$$

and

$$E_B(x) = E_{B_\infty} - \frac{\nu q_0}{2\varepsilon_2 x} \tag{21}$$

where

$$E_{B_\infty} = \frac{q_0}{\varepsilon_2 r_c} + \frac{q_0}{\varepsilon_c}\left(\frac{1}{r_i} - \frac{1}{r_c}\right) \tag{22}$$

$$q_0 = \frac{1}{4\pi\varepsilon_0}\frac{e_o^2}{2kT} = 283\,\text{Å} \quad \text{at } 22.5\,^\circ\text{C} \tag{23}$$

$$\nu = \frac{\varepsilon_1 - \varepsilon_2}{\varepsilon_1 + \varepsilon_2}. \tag{24}$$

[5] The expression of $E_B(x)$ assumes the complex can be considered in a semi-infinite medium. This assumption is equivalent to neglecting the image forces from the other interface, which is well justified in the cases that will be studied here where x is small compared to the membrane thickness. Moreover, Eq. (21) will be used solely to compare carriers and since in this comparison, only differences in $E_B(x)$ will be considered, the eventual small correction will practically vanish.

In the above expressions, ε_0 is the free space permittivity, e_o, the electronic charge, k, the Boltzman constant, and T, the absolute temperature. We then obtain for the ratio of the rates of transfer of two complexes with the same ion.

$$\frac{k_{is}^1}{k_{is}^2} = \exp\frac{\nu q_o}{2\varepsilon_2}\left(\frac{1}{x_2} - \frac{1}{x_1}\right). \tag{25}$$

This relation shows that the larger is the distance between the center of the complex and the interface, the larger is k_{is}. This is a very interesting finding since, in order to explain the observed increase of k_{is} with carrier size, we only have to postulate that the edge of the complex coincides with the interface or that the adsorption distance corresponds to the carrier radius. Although the individual radii for the different carriers are not available, except for nonactin for which it is 6.3 Å (Simon & Morf, 1973), so that a quantitative prediction for the variation of k_{is} is not possible, we can, however, do the inverse calculation, namely, start from the known increase in k_{is} and see if the increase in carrier radius is reasonable. Performing the calculation with the values of k_{is} for NH_4^+ from Table 2, using $\varepsilon_1 = 78$ and $\varepsilon_2 = 2$, we obtain for the radii of the different homologues, the values of x_h that appear in the second row of Table 7. We see that from nonactin to tetranactin, the increase in radius needs be only 1.1 Å in order to be compatible with the observed increase in k_{is}. Considering that the covalent diameter of an additional carbon from CPK models is 1.55 Å and that for tetranactin, four of these are distributed symmetrically around the molecule, this increase appears quite acceptable since due to motion of the complex, the interface will see more or less an average radius. Moreover, and interestingly, we will see that the above hypothesis will allow us to predict the variations in k_{Di} with methylation from the corresponding variations in k_{is}.

k_{Di}

Table 2 shows that k_{Di} decreases strongly with methylation and at a rate somewhat greater than that of the increase in k_{is}. This phenomenon is much less pronounced in bulk phases such as a methanol-chloroform mixture (Grell, Funck & Eggers, 1975) where the overall dissociation rate constant decreases by a factor of only 1.5 from nonactin to trinactin, while we observe a factor 3.5; we might again seek the explanation in terms of electrostatic energy barriers. Figure 6 represents the potential energy barriers encountered by an ion when crossing the membrane from one aqueous phase to the other

Table 7. Radii of complexes of nonactin homologues according to Eq. (25)

	Non[a]	Mon	Din	Trin	Tetran
k_{is}^n/k_{is}^n [b]	1	1.78	2.71	3.14	5.03
x_n (Å)	6.3	6.65	6.94	7.04	7.4

[a] The value for nonactin is assumed from Simon and Morf (1973).
[b] Ratio of k_{is} for a given homologue to that of nonactin.

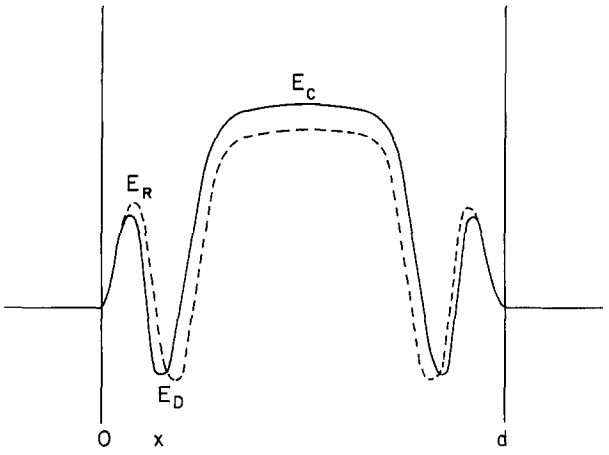

Fig. 6. Potential energy profiles for an ion and a carrier crossing a membrane from one aqueous phase to the other. Profiles for two hypothetical carriers of different size with the same ion. Within the present framework, the fact that with a larger carrier (dashed line) the ion is located further away from the interface is responsible for the lower decrease in E_D as compared to that in E_C (*cf.* Eqs. (20) and (21)). This combined with the constancy of E_R with carrier, is at the origin of the relationship between k_{is} and k_{Di} (*cf.* Eq. (26))

with two hypothetical carriers of different size. E_R represents the energy peak for formation of the ion-carrier complex, E_D is the energy of the formed complex at the adsorption site and E_C is the energy peak for translocation of the complex, E_D and E_C corresponding to $E_B(x)$ and $E_B(d/2)$, respectively. Accordingly, assuming as before, that the distance of the center of the carrier from the interface corresponds to its radius, and considering that k_{Ri} seems quite invariant from one homologue to the other, we find, with the help of Eqs. (20) through (25)

$$(k_{Di}^1/k_{Di}^2)=(k_{is}^1/k_{is}^2)^{1-2/\nu}=(k_{is}^1/k_{is}^2)^{-1.1} \tag{26}$$

where we have used as before $\varepsilon_1=78$, $\varepsilon_2=2$, and assumed $\varepsilon_c \gg \varepsilon_2$.

Table 8 shows the test of Eq. (26) for NH_4^+, K^+, Rb^+, and Tl^+ ions using the values of k_{is} and k_{Di} from Table 2. We see that, although the values for k_{Di} vary by a factor of one hundred from the NH_4^+-tetranactin complex to the Tl^+-nonactin complex, the predictions of Eq. (26) are fairly well verified. As a matter of fact, the few deviations that are observed can be directly correlated with a larger uncertainty in the values of the rate constants (*cf.* $\bar{\Delta}$%, Table 2). It should be realized that the ability of Eq. (26) to predict the variation of k_{Di} from that of k_{is}, results directly from our assumption according to which the position of the energy minimum from the interface at the adsorption site corresponds to the radius of the carrier.

Table 8. Test of the prediction of Eq. (26)

	NH_4^+		K^+		Rb^+		Tl^+	
	I	II	I	II	I	II	I	II
Tetran	0.59	0.45	0.5	0.28	0.43	0.54	0.4	0.4
Trin	1.0	1.0	1.0	1.0	1.0	1.0	1.0	1.0
Din	1.18	1.5	1.28	1.91	1.08	2.94	1.47	1.46
Mon	1.87	2.2	1.36	3.01			3.35	3.24
Non	3.52	3.52					4.1	8.44

I: $(k_{is}^1/k_{is}^2)^{-1.1}$ calculated relative to trinactin.
II: k_{Di}^1/k_{Di}^2 relative to trinactin.

Obviously, from one homologue to the other, other factors might influence the energy of the complex at the adsorption site or in the middle of the membrane, and consequently k_{is} and k_{Di}, such as variation in the free carrier energy profile or membrane surface dipoles, variation of the dielectric constant near the interface or change in dipolar moment of the coordinating ligands of the molecule. Unfortunately, however, their importance cannot be as easily assigned at the present time.

k_s

Table 2 shows that the rate of transfer of the free carrier, k_s, does not change with carrier methylation and that its value is close to $7\times10^4\,\mathrm{sec}^{-1}$. This is 25 times larger than the value of k_{is} for nonactin and only five times larger than that for tetranactin. However, assuming that the complex and the carrier have similar conformations inside the membrane, i.e., the same covalent radius, one would expect from Eqs. (20) and (21) the energy barrier for the nonactin complex to be $6.9\,kT$ higher than that for the free nonactin molecule and the free nonactin to move nearly one thousand times faster than its complex. This discrepancy could find a satisfactory explanation if the free carrier would be adsorbed to the membrane interface with the carbonyl groups oriented towards and close to the aqueous phase and the apolar parts oriented towards the membrane interior in a way similar to that proposed for valinomycin

by Shemyakin et al. (1969) and as discussed by Stark et al. (1971) and Haydon and Hladky (1972). Therefore, the free carrier would also have to surmount an electrostatic energy barrier in desorbing from the interface, and this desorption which would then become the rate-limiting step for the rate of transfer of the carrier would therefore be independent of the carrier methylation as is observed.

k_{Ri}

As discussed previously and as can be seen in Table 2, k_{Ri} seems to be an invariant, first as a function of carrier methylation, and also as a function of ion with the exception of Tl^+ ion; the variations are small and probably more related to the level of imprecision in the determination than to any fundamental differences. In fact, the values we find for k_{Ri} are about three orders of magnitude lower than those reported for methanol solutions, for which they appear to be diffusion controlled (Grell et al., 1975), clearly indicating that the membrane interface offers an additional barrier to the complexation reaction. Therefore it would be very unlikely that methylation could modulate this rate-limiting step. As far as the variations of k_{Ri} with ion are concerned, we might consider that NH_4^+, K^+, and Rb^+ have nearly the same crystal radii, so that they are likely to see the same energy barrier when crossing the interface and reaching the carrier in its open configuration. This could then well explain why k_{Ri} is the same for these three ions. The higher value of k_{Ri} by a factor five observed for all homologues with Tl^+, which has, however, a crystal radii in between that of Rb^+ and K^+, is probably related to its particular feature of being a polarizable ion. So, from one ion to the other, with the exception of Tl^+, we would expect the equilibrium constant ($\bar{K}_i$) for the heterogenous reaction to be controlled by the dissociation constant k_{Di}. This prediction related to the constancy of k_{Ri} can be easily checked since a reliable value of the ratio ($\bar{K}_i/\bar{K}_j$) can be obtained directly from the ratio of the equilibrium extraction constants (K_i/K_j) of these metal ion salts in organic solvents (Eisenman et al., 1969). Therefore, we have

$$\frac{K_i}{K_j} = \frac{\bar{K}_i}{\bar{K}_j} = \frac{k_{Ri}}{k_{Rj}} \frac{k_{Dj}}{k_{Di}} \simeq \frac{k_{Dj}}{k_{Di}}. \tag{27}$$

Table 9 shows the comparison of these two ratios with respect to K^+ for monactin, dinactin, and trinactin. The values of (K_j/K_{K^+}) are taken from Table 15 of Eisenman et al. (1969) and the ratios (k_{DK^+}/k_{Dj}) from Table 2. It can be seen that, although the individual values of k_{Di} vary by more than a factor 30, the predictions of Eq. (27) are followed well within a factor 2. This finding stresses the importance of the step of dissociation of the complex in determining the equilibrium selectivity of carrier molecules.

Table 9. Comparison of the ratios k_{Dj}/k_{Di} with the ratios of the extraction equilibrium constant in organic solvents K_i/K_j

	Mon		Din		Trin	
	I	II	I	II	I	II
NH_4^+	9.2	19	9.2	12	7.2	12
K^+	1.0	1.0	1.0	1.0	1.0	1.0
Rb^+			0.25	0.40	0.39	0.29

I: k_{Dj}/k_{Di} with respect to K^+.
II: K_i/K_j with respect to K^+. From Eisenman et al., 1969, Table 15.

γ_s and Γ_s

We have seen in Table 6 that γ_s changes by only a factor three from nonactin to tetranactin. As discussed by Benz and Stark (1975), assuming a contribution of 500 cal/mole for each CH_2 group, one would have expected γ_s for tetranactin to be about 30 times larger than for nonactin. However, this type of reasoning based on molecule surface considerations, if justified and verified in the case of straight or branched molecules for which each additional group is exposed to the solvent, is quite questionable for large spherical molecules such as the macrotetralides. Indeed, although four ethyl groups are added to the tetranactin molecules, they are likely to be more or less embedded beneath the four terminal methyl groups, so that they cannot interact completely with the neighboring solvent molecules and consequently cannot exhibit the full predicted change in free energy. We would then expect, as observed, a lower increase in γ_s.

Γ_s, in the present model, reflects the equilibrium number of carrier molecules in the membrane available for complexation with ions in the aqueous phase and therefore the membrane carrier concentration near the interface. From Table 6, we see that Γ_s is larger than unity which thus indicates that the free carrier interacts more with the membrane than with the mostly decane bulk phase of the torus. This finding would be compatible with the idea proposed above that the carrier is adsorbed near the interface, its polar groups oriented towards the aqueous phase providing the additonal interaction energy. The variations in Γ_s with increasing methylation are quite small as expected since they reflect mostly changes in interaction energy of the hydrophobic exterior of the carrier molecule within two very similar hydrocarbon phases.

Comparison with Glyceryl-Dioleate (GDO) Bilayers

A good amount of kinetic data has been already reported on so-called glyceryl-dioleate/decane bilayers (Laprade et al., 1975; Krasne & Eisenman, 1976); although the lipid used was not pure (90% purity mixture of 1-2 and 1-3 esters from Pfaltz and Bauer) and probably contained a good amount of monoolein, it would be interesting to compare the rate constants obtained on this lipid with those obtained on monoolein. Table 10 presents the values of the rate constants obtained with trinactin and NH_4^+, K^+, and Tl^+ ions on GDO bilayers. These have been calculated from the data of Laprade et al. (1975) using the same procedure we have used in the present work. Interestingly, the values in Table 10 are very close to those calculated by Laprade et al. (1975) using also a curve-fitting procedure but including, in addition, steady-state current-voltage and zero-current potential data. Comparing the values in Table 10 with the corresponding ones in Table 2, we may conclude that they are nearly identical. So, from the above evidence as far as the carrier mechanism is concerned, this so-called GDO/decane bilayer is identical to a monoolein/decane one.

Table 10. Rate constants for trinactin on GDO bilayers

	NH_4^+	K^+ [a]	Tl^+
k_{is}	5.5×10^3	9.7×10^3	1.1×10^4
k_s	5.8×10^4		1.4×10^5
k_{Ri}	8.8×10^4		1.8×10^6
k_{Di}	1.0×10^4	5.2×10^4	5.7×10^4

[a] For K^+, the relaxation data was not sufficient to allow a reliable determination of k_s and k_{Ri}.

We gratefully acknowledge Dr. K. Ando and Dr. W. Simon for the gifts of tetranactin and Dr. Hans Bickel and Ms. Barbara Stearns for the gifts of nonactin, monactin, dinactin, and trinactin. In addition, we thank Dr. Garbor Szabo and Dr. Rémy Sauvé for many helpful discussions as well as for critically reading this manuscript. Finally, we are very grateful to Ms. Louise Lefort for her competent and dedicated secretarial work.

This work was supported by the CRSNG Canada and by the FCAC Québec.

Appendix A

Determination of Rate Constants Taking into Account Their Voltage Dependence

Although a theory for relaxations taking into account the voltage dependence of the rate constants over the actual experimental range of applied voltages has still to be worked out, it is, however, possible to estimate the voltage-independent portion of some rate constants or their combinations from voltage-jump relaxation experiments conducted at small applied potentials (Hladky, 1979*b*). Indeed, since in our case, at least at low applied potentials, $\alpha_{obs}=\alpha_T$, the expression for α_T is given by (Markin & Liberman, 1973; Hladky, 1979*a*, *b*)

$$\alpha_T+1=\left(1+\frac{2k_{is}}{k_{Di}}+\frac{k_{Ri}c_i k_{is}}{k_{Di}k_s}\right)\left[\gamma^2+\frac{k_{Di}}{2k_{is}}(2\xi)^2\right] \tag{A1}$$

where γ and ξ are related by $2\xi+\gamma=1$.

ξ represents the equivalent of charge transported across the membrane whenever an ion binds to a carrier on the left or a complex dissociates on the right, while γ corresponds to the equivalent of charge transported when a complex crosses the membrane. The value of ξ is obtained from the potential dependence of $(k'_{is}+k''_{is})$ as measured by changes in τ_{obs} (Hladky, 1975*b*). Indeed, since in all cases here the slower relaxation dominates, we have

$$(k'_{is}+k''_{is})=\frac{1}{\tau}\frac{\alpha}{\alpha+1} \tag{A2}$$

Table 11. Rate constants in the limit of low applied voltage, considering the voltage dependence of the rate constants[a]

	NH_4^+				
	Non	Mon	Din	Trin	Tetran
k_{is} (sec^{-1})	4.1×10^3	6.2×10^3	9.4×10^3	9.9×10^4	1.6×10^4
k_{Di} (sec^{-1})	1.3×10^4	1.0×10^4	8.7×10^3	5.1×10^3	2.2×10^3
k_{Ri}/k_s (M^{-1})	2.7	2.73	4.38	2.22	1.91
	Tetran				
	K^+		Rb^+		Tl^+
k_{is} (sec^{-1})	1.9×10^4		2.1×10^4		1.5×10^4
k_{Di} (sec^{-1})	1.1×10^4		4.0×10^4		7.4×10^3
k_{Ri}/k_s (M^{-1})	1.67		1.94		2.81

[a] The same value of $\xi=0.095$ was used for all carriers.

where τ and α corresponds to τ_{obs} and α_{obs}, respectively, and k'_{is} and k''_{is} are given by

$$k'_{is} = k_{is} \exp[-(0.5-\xi) F \Delta V/RT] \quad (A3)$$

$$k''_{is} = k_{is} \exp[(0.5-\xi) F \Delta V/RT]. \quad (A4)$$

As was found by Hladky (1975*b*), no significant variations in the value of ξ as a function of the carrier or the ion was seen, so the same value of $\xi = 0.095$ was used to obtain k_{is} from Eq. (A2) for all ion-carrier combinations[6]. From the value of α_T as a function of ion activity which in our case is equal to α_{obs} and the value of ξ, it is possible to obtain the ratios k_{is}/k_{Di} and k_{Ri}/k_s. Then from the above calculated value of k_{is} we can obtain k_{Di}.

Table 11 summarizes the results of such a procedure applied to our data obtained at 10 mV with NH_4^+ for the whole series of homologues and with tetranactin for NH_4^+, K^+, Rb^+, and Tl^+ ions. If we compare these values to the corresponding ones in Table 2, we can see that for all ion-carrier combinations, the values of k_{is} in Table 11 are between about 10 and 20% larger than those in Table 2 while the values of k_{Di} are about two times smaller; the values of the ratio k_{Ri}/k_s is relatively unchanged except maybe for Tl^+ where it is significantly decreased. However, it should be emphasized that, although the absolute values of k_{is} and k_{Di} are slightly altered, the same trends as a function of carrier methylation or as a function of the ion that were seen in Table 2, are seen in Table 11: k_{is} and k_{Di} vary by about the same factors from nonactin to tetranactin, while from one ion to the other, k_{is} remains about the same and k_{Di} varies by about the same factor. Consequently, the values in Table 11 would agree as well as those of Table 2 with the predictions of Eqs. (25) and (26).

[6] It should be pointed out here that ξ being invariant with carrier is not really in contradiction with the concept introduced in the discussion according to which the wells are not located at the same distance from the interface for the different carriers. Indeed, we needed only 1 Å to explain the change in k_{is}, so that for a membrane of 50 Å the effect on the voltage dependence of the rate constants would be barely noticeable.

Appendix B

Observed Time Constants and Amplitudes of Relaxation[a]

Table B1. Tetranactin

	V (mV)	τ_{obs} (μsec)				α_{obs}			
	c_i (M)	0.01	0.1		1	0.01	0.1		1
	c_s^a (M)	5×10^{-8}	2×10^{-8}		5×10^{-9}	5×10^{-8}	2×10^{-8}		5×10^{-9}
K^+	10	16.6	18.8		22.2	2.3	2.1		4.2
	25	15.8	18.4		20.9	2.4	2.3		4.3
	50	14.3	15.4		17.4	2.8	2.9		5.2
	100	9.1	9.5		9.8	5.6	4.9		11.6
	150	(3.5)[b]	(5.7)			(13.6)	(11.7)		
	c_i (M)	0.01	0.1		1	0.01	0.1		1
	c_s^a (M)	5×10^{-8}	1.5×10^{-8}		10^{-8}	5×10^{-8}	1.5×10^{-8}		10^{-8}
Rb^+	10	7.4	7.6		11.4	0.49	0.52		1.2
	25	7.7	7.3		12.7	0.56	0.59		1.3
	50	7.3	7.3		10.0	0.57	0.69		1.6
	100	6.0	6.1		6.6	1.1	1.3		3.4
	150	(4.7)	(4.1)		(4.3)	(1.1)	(3.2)		(6.5)
	c_i (M)	0.01	0.1	0.5	1	0.01	0.1	0.5	1
	c_s^a (M)	1.6×10^{-8}	1.6×10^{-8}	1.6×10^{-8}	2×10^{-8}	1.6×10^{-8}	1.6×10^{-8}	1.6×10^{-8}	2×10^{-8}
Tl^+	10	18.1	21.3	30.6	37.6	1.7	2.44	4.2	5.8
	25	16.9	20.0	29.7	35.2	2.0	3.12	4.8	6.7
	50	15.4	16.1		28.5	2.8	5.10		7.9
	100	10.2	11.3		15.4	8.9	16.4		22.7

[a] These values are generally the mean of three different measurements. For the greater majority of the data, the scatter between extreme values was well within 15% of the mean. As expected, in the case of both short time constant and small amplitude relaxations, the scatter was slightly more important due to experimental limitations.

[b] Values in parentheses have not been included in the final curve-fitting program because they might have corresponded to the faster relaxation process (τ_2, α_2).

Table B2. Trinactin

	V (mV)	τ_{obs}				α_{obs}			
	c_i (M)	0.01	0.1	0.3	1	0.01	0.1	0.3	1
	c_s^a (M)	5×10^{-8}	2×10^{-8}	10^{-8}	10^{-8}	5×10^{-8}	2×10^{-8}	10^{-8}	10^{-8}
K^+	25	10.6	12.1	14.9	20.2	0.39	0.53	0.69	1.0
	50	10.6	11.8	13.2	17.0	0.47	0.59	0.82	1.3
	75	9.8	10.0	11.5	13.8	0.62	0.82	1.0	1.6
	100	8.3	8.3	9.8	11.0	0.88	1.1	1.4	2.3
	125	6.8	6.8	7.8	8.4	1.2	1.5	1.8	3.3
	150	5.8	5.7	6.4	6.7	1.6	2.1	2.4	4.3
	c_i (M)		0.1	0.3	1		0.1	0.3	1
	c_s^a (M)		5×10^{-8}	2×10^{-8}	2×10^{-8}		5×10^{-8}	2×10^{-8}	2×10^{-8}
Rb^+	10				11.5				0.21
	25			8.5	11.6			0.15	0.21
	50		8.4	8.5	10.8		0.08	0.18	0.27
	75		8.4	7.8	9.8		0.09	0.21	0.35
	100		8.4	6.9	8.5		0.11	0.26	0.47
	125		7.2	6.1	7.3		0.14	0.36	0.64
	150		6.1	5.4	6.0		0.18	0.43	0.84
	c_i (M)	0.01	0.1		1	0.01	0.1		1
	c_s^a (M)	2×10^{-8}	2.5×10^{-9}		2.5×10^{-9}	2×10^{-8}	2.5×10^{-9}		2.5×10^{-9}
Tl^+	10	15.0	22.7		41.6	0.33	0.63		1.4
	25	12.9	21.9		39.9	0.35	0.71		1.4
	50	13.0	20.1		35.2	0.39	0.89		1.6
	100	12.0	14.9		24.6	0.52	1.7		3.1
	150	9.3	10.2			0.90	4.5		

Table B3. Dinactin

	V (mV)	τ_{obs}					α_{obs}				
	c_i (M)	0.01	0.1		0.5	1	0.01	0.1		0.5	1
	c_s^a (M)	10^{-8}	5×10^{-9}		5×10^{-9}	5×10^{-9}	10^{-8}	5×10^{-9}		5×10^{-9}	5×10^{-9}
NH_4^+	10	33.3	34.8		39.4	40.1	1.3	1.6		2.9	4.2
	25	31.9	33.2		36.5	36.5	1.4	1.7		3.3	4.6
	50	27.8	28.9		31.5	30.3	1.7	2.3		4.2	5.7
	100	18.3	19.2		19.5	18.4	3.9	4.1		8.4	11.6
	150	8.3	10.3		10.8	9.5	(19.1)	(14.2)		24.3	34.5
	c_i (M)	0.01	0.1	0.3		1	0.01	0.1	0.3		1
	c_s^a (M)	2×10^{-7}	4×10^{-8}	2×10^{-8}		10^{-8}	2×10^{-7}	4×10^{-8}	2×10^{-8}		10^{-8}
K^+	10					14.5					0.35
	25			11.1		15.2			0.21		0.56
	50	8.0	9.5	11.0		14.7	0.10	0.11	0.25		0.66
	75	7.7	9.5	11.0		12.8	0.12	0.13	0.30		0.93
	100	8.2	9.6	10.9		10.4	0.14	0.17	0.34		1.4
	125	8.3	9.3	9.9		8.6	0.17	0.20	0.49		2.0
	150	8.1	8.5	8.8		7.0	0.21	0.26	0.69		3.0
	c_i (M)		0.1	0.3	0.5	1		0.1	0.3	0.5	1
	c_s^a (M)		10^{-7}	5×10^{-8}	6×10^{-8}	2.5×10^{-8}		10^{-7}	5×10^{-8}	6×10^{-8}	2.5×10^{-8}
Rb^+	25					10.0					0.08
	50			9.2	10.1	10.2			0.03	0.05	0.10
	75		8.3	8.9	9.3	9.5		0.04	0.04	0.07	0.15
	100			7.7	7.8	8.5			0.06	0.11	0.23
	125		6.5	6.6	7.4	7.4		0.04	0.08	0.19	0.33
	150		6.1	5.6	7.3	6.6		0.05	0.15	0.25	0.61
	c_i (M)	0.01	0.1			1	0.01	0.1			1
	s_s^a (M)	10^{-7}	10^{-7}			10^{-7}	10^{-7}	10^{-7}			10^{-7}
Tl^+	10	12.5	17.2			40.4	0.20	0.24			0.65
	25	12.1	18.5			38.6	0.22	0.24			0.74
	50	13.2	19.4			36.8	0.23	0.28			0.87
	100	11.9	17.1			25.4	0.42	0.54			1.8
	150	9.5	12.2			14.7	1.5	1.2			4.4

Table B4. Monactin

	V (mV)	τ_{obs}					α_{obs}				
	c_i (M)	0.01	0.1	0.5	1		0.01	0.1	0.5	1	
	c_s^a (M)	5×10^{-8}	10^{-8}	10^{-8}	10^{-8}		5×10^{-8}	10^{-8}	10^{-8}	10^{-8}	
NH_4^+	10	29.6	35.2	40.7	44.9		0.56	0.58	1.2	1.6	
	25	29.0	34.8	39.1	45.6		0.61	0.66	1.3	1.7	
	50	26.1	30.4	35.4	40.4		0.84	0.88	1.6	2.1	
	100	19.0	20.6	26.6	27.3		1.7	1.9	2.7	4.0	
	150	11.9	12.5	16.0	16.3		5.3	5.0	6.4	9.0	
	c_i (M)	0.01	0.1		1	3	0.01	0.1		1	3
	c_s^a (M)	5×10^{-7}	2×10^{-8}		4×10^{-9}	5×10^{-9}	5×10^{-7}	2×10^{-8}		4×10^{-9}	5×10^{-9}
K^+	10					13.9					0.45
	25				7.2	15.0				0.13	0.43
	50	6.4	8.0		8.9	11.2	0.08	0.13		0.33	0.68
	100	4.9	5.2		7.7	9.5	0.19	0.32		0.64	0.79
	150	4.0	4.6		6.5	6.8	0.46	0.56		1.0	1.8
	c_i (M)	0.01	0.1	0.3	1		0.01	0.1	0.3	1	
	c_s^a (M)	2×10^{-7}	2×10^{-8}	2.5×10^{-8}	5×10^{-8}		2×10^{-7}	2×10^{-8}	2.5×10^{-8}	5×10^{-8}	
Tl^+	25			19.5	42.0		0.07		0.16	0.31	
	50	9.3	13.7	19.5	37.9		0.08	0.08	0.24	0.35	
	75	7.7	13.9	19.6	33.0		0.10	0.10	0.33	0.56	
	100	9.1	14.8	18.5	30.3		0.12	0.13	0.48	0.72	
	125	6.7	14.3	17.0	24.3		0.19	0.19	0.62	1.06	
	150	9.0	12.9	15.5	20.2		0.24	0.25	0.79	1.44	

Table B5. Nonactin

	V (mV)	τ_{obs}					α_{obs}				
	c_i (M)	0.01	0.1	0.5	1		0.01	0.1	0.5	1	
	s_s^a (M)	3×10^{-7}	2×10^{-8}	10^{-8}	10^{-8}		3×10^{-7}	2×10^{-8}	10^{-8}	10^{-8}	
NH_4^+	10	26.8	34.9	33.9	63.2		0.14	0.26	0.45	0.69	
	25	25.2	30.5	37.8	52.2		0.17	0.32	0.47	0.80	
	50	23.0	28.7	34.9	46.6		0.25	0.44	0.65	1.1	
	100	16.9	21.0	25.6	31.9		0.61	0.96	1.4	2.1	
	150	13.2	14.1	16.1	19.8		1.74	3.04	3.3	4.6	
	c_i (M)		0.1	0.3	1	3		0.1	0.3	1	3
	c_s^a (M)		2×10^{-7}	5×10^{-8}	4×10^{-8}	5×10^{-8}		2×10^{-7}	5×10^{-8}	4×10^{-8}	5×10^{-8}
K^+	10					10.1					0.17
	25				9.0	10.6				0.07	0.17
	50			9.1	9.6	10.6			0.05	0.09	0.20
	75			9.4					0.05		
	100		9.3	9.1	8.3	8.3		0.04	0.04	0.12	0.42
	125		8.5					0.04			
	150				5.8	6.4				0.26	0.88
	c_i (M)		0.1		1			0.1		1	
	c_s^a (M)		2×10^{-7}		2×10^{-8}			2×10^{-7}		2×10^{-8}	
Tl^+	10				13.6					0.07	
	25				13.2					0.07	
	50		12.9		12.8			0.019		0.08	
	100		14.3		12.8			0.029		0.15	
	150		13.6		10.2			0.10		0.32	

References

Benz, R. 1978. Alkali ion transport through lipid bilayer membranes mediated by enniatin A and B and beauvericin. *J. Membrane Biol.* **43**:367–394

Benz, R., Frölich, O., Läuger, P., Montal, M. 1975. Electrical capacity of black lipid films and of lipid bilayers formed from monolayers. *Biochim. Biophys. Acta* **394**:323–334

Benz, R., Läuger, P. 1976. Kinetic analysis of carrier-mediated ion transport by the charge-pulse technique. *J. Membrane Biol.* **27**:171–191

Benz, R., Stark, G. 1975. Kinetics of macrotetralide-induced ion transport across lipid bilayer membranes. *Biochim. Biophys. Acta* **382**:27–40

Benz, R., Stark, G., Janko, K., Läuger, P. 1973. Valinomycin-mediated ion transport through neutral lipid membranes: In-

fluence of hydrocarbon chain length and temperature. *J. Membrane Biol.* **14**:339–364

Ciani, S.M., Eisenman, G., Laprade, R., Szabo, G. 1973*a*. Theoretical analysis of carrier-mediated electrical properties of bilayer membranes. *In:* Membranes – A Series of Advances. G. Eisenman, editor. Vol. 2, pp. 61–177. Marcel Dekker, New York

Ciani, S., Laprade, R., Eisenman, G., Szabo, G. 1973*b*. Theory for carrier-mediated zero-current conductance of bilayers extended to allow for nonequilibrium of interfacial reactions, spatially dependent mobilities and barrier shape. *J. Membrane Biol.* **11**:255–292

Eisenman, G., Ciani, S.M., Szabo, G. 1968. Some theoretically expected and experimentally observed properties of lipid bilayer membranes containing neutral molecular carriers of ions. *Fed. Proc.* **27**:1289–1304

Eisenman, G., Ciani, S., Szabo, G. 1969. The effects of the macrotetralide actin antibiotics on the equilibrium extraction of alkali metal salts into organic solvents. *J. Membrane Biol.* **1**:294–345

Eisenman, G., Szabo, G., Ciani, S., McLaughlin, S.G.A., Krasne, S. 1973. Ion binding and ion transport produced by lipid soluble molecules. *Prog. Surf. Membr. Sci.* **6**:139–241

Feldberg, S.W., Kissel, G. 1975. Charge pule studies of transport phenomena in bilayer membranes: I. Steady-state measurements of actin- and valinomycin-mediated transport in glycerol monooleate bilayers. *J. Membrane Biol.* **20**:269–300

Fettiplace, R., Andrews, D.M., Haydon, D.A. 1971. The thickness, composition, and structure of some lipid bilayers and natural membranes. *J. Membrane Biol.* **5**:277–296

Gambale, F., Gliozzi, A., Robello, M. 1973. Determination of rate constants in carrier-mediated diffusion through lipid bilayers. *Biochim. Biophys. Acta* **330**:325–334

Grell, E., Funck, T., Eggers, F. 1975. Structure and dynamic properties of ion-specific antibiotics. *In:* Membranes – A Series of Advances. G. Eisenman, editor. Vol. 3, pp. 1–126. Marcel Dekker, New York

Grunwald, E.G., Baughman, G., Kohnstam, G. 1960. The solvation of electrolytes in dioxane water mixtures, as deduced from the effect of solvent change on the standard partial molar free energy. *J. Am. Chem. Soc.* **82**:5801–5811

Haydon, D.A., Hladky, S.B. 1972. Ion transport across thin lipid membranes: A critical discussion of mechanisms in selected systems. *Q. Rev. Biophys.* **5**:187–282

Hladky, S.B. 1972. The steady-state theory of the carrier transport of ions. *J. Membrane Biol.* **10**:67–91

Hladky, S.B. 1973. The effect of stirring on the flux of carriers into black lipid membranes. *Biochim. Biophys. Acta* **307**:261–269

Hladky, S.B. 1975*a*. Steady-state ion transport by nonactin and trinactin. *Biochim. Biophys. Acta* **375**:350–362

Hladky, S.B. 1975*b*. Tests of the carrier model for ion transport by nonactin and trinactin. *Biochim. Biophys. Acta* **375**:327–349

Hladky, S.B. 1979*a*. Ion transport and displacement currents with membrane bound carriers. *J. Membrane Biol.* **46**:213–237

Hladky, S.B. 1979*b*. The carrier mechanism. *Curr. Top. Membr. Transp.* **12**:53–164

Knoll, W., Stark, G. 1975. An extended kinetic analysis of valinomycin-induced Rb-transport through monoglyceride membranes. *J. Membrane Biol.* **25**:249–270

Krasne, S., Eisenman, G. 1976. Influence of molecular variations of ionophore and lipid on the selective ion permeability of membranes. I. Tetranactin and the methylation of nonactin-type carriers. *J. Membrane Biol.* **30**:1–44

Laprade, R., Ciani, S.M., Eisenman, G., Szabo, G. 1975. The kinetics of carrier-mediated ion permeation in lipid bilayers and its theoretical interpretation. *In:* Membranes – A Series of Advances. G. Eisenman, editor. Vol. 3, pp. 127–214. Marcel Dekker, New York

Laprade, R., Grenier, F., Asselin, S. 1978. Influence of methylation of ionophore on the kinetics of carrier-mediated ion transport in lipid bilayers. Abstracts, 6th Int. Biophysics Congress, Kyoto, p. 361

Laprade, R., Grenier, F., Asselin, S. 1979. Measurement of lateral diffusion coefficient of ion carriers in lipid bilayers using conductance measurements. *Biophys. J.* **25** (2):180*A*

Läuger, P., Stark, G. 1970. Kinetics of carrier-mediated ion transport across lipid bilayer membranes. *Biochim. Biophys. Acta* **211**:458–466

Markin, V.S., Kristalik, L.I., Liberman, E.A., Topaly, V.P. 1969. Cell biophysics. Mechanism of conductivity of artificial phospholipid membranes in the presence of ion carriers. *Biofizika* 2 **14**:256–264

Markin, V.S., Liberman, Y.A. 1973. Transitional current on voltage clamping of a membrane with an ion carrier. Theory. *Biophysics* **18**:475–482

Mueller, P., Rudin, D.O. 1967. Development of $K^+ - Na^+$ discrimination in experimental bimolecular lipid membranes by macrocyclic antibiotics. *Biochem. Biophys. Res. Commun.* **26**:398–404

Neumcke, B., Läuger, P. 1969. Nonlinear electrical effects in lipid bilayer membranes: II. Integration of the generalized Nernst-Planck equations. *Biophys. J.* **9**:1160–1170

Parsegian, A. 1969. Energy of an ion crossing a low dielectric membrane: Solutions to four relevant electrostatic problems. *Nature (London)* **221**:844–846

Pressman, B.C., Harris, E.J., Jaeger, W.S., Johnson, J.H. 1967. Antibiotic-mediated transport of alkali ions across lipid barriers. *Proc. Natl. Acad. Sci. USA* **58**:1949–1956

Shemyakin, M.M., Ovchinikov, Yu.A., Ivanov, V.T., Antonov, V.K., Vinogradova, E.I., Shkrob, A.M., Malenkov, G.G., Evstratov, A.V., Laine, I.A., Melnik, E.I., Ryabova, I.D. 1969. Cyclodepsipeptides as chemical tools for studying ionic transport through membranes. *J. Membrane Biol.* **1**:402–430

Simon, W., Morf, W.E. 1973. Alkali cation specificity of carrier antibiotics and their behavior in bulk membranes. *In:* Membranes – A Series of Advances. G. Eisenman, editor. Vol. 2, p. 329–375. Marcel Dekker, New York

Skinner, J.F., Fuoss, R.M. 1964. Conductance of triisoamylbutylammonium and tetraphenylboride. *J. Phys. Chem.* **68**:1882–1885

Stark, G., Benz, R. 1971. The transport of potassium through lipid bilayer membranes by the neutral carriers valinomycin and monactin. *J. Membrane Biol.* **5**:133–153

Stark, G., Ketterer, B., Benz, R., Läuger, P. 1971. The rate constants of valinomycin mediated ion transport through thin lipid membranes. *Biophys. J.* **11**:981–984

Szabo, G., Eisenman, G., Ciani, S. 1969. The effects of the macrotetralide actin antibiotics on the electrical properties of phospholipid bilayer membranes. *J. Membrane Biol.* **1**:346–382

Szabo, G., Eisenman, G., Ciani, S.M., Laprade, R., Krasne, S. 1973. Experimentally observed effects of carriers on the electrical properties of membranes. The equilibrium domain. *In:* Membranes – A Series of Advances. G. Eisenman, editor. Vol. 2, pp. 179–328. Marcel Dekker, New York

Tosteson, D.C. 1968. Effect of macrocyclic compounds on the ionic permeability of artificial and natural membranes. *Fed. Proc.* **27**:1269–1277

White, S.H. 1973. The surface charge and double layers of thin lipid films formed from neutral lipids. *Biochim. Biophys. Acta* **323**:343–350

Received 1 May 1981; revised 23 December 1981